

Efficient Representation of Quantum Many-body States with Deep Neural Networks

Xun Gao¹ and Lu-Ming Duan^{1,2}

¹Center for Quantum Information, IIIS, Tsinghua University, Beijing 100084, PR China

²Department of Physics, University of Michigan, Ann Arbor, Michigan 48109, USA

The challenge of quantum many-body problems comes from the difficulty to represent large-scale quantum states, which in general requires an exponentially large number of parameters. Recently, a connection has been made between quantum many-body states and the neural network representation (*arXiv:1606.02318*). An important open question is what characterizes the representational power of deep and shallow neural networks, which is of fundamental interest due to popularity of the deep learning methods. Here, we give a rigorous proof that a deep neural network can efficiently represent most physical states, including those generated by any polynomial size quantum circuits or ground states of many-body Hamiltonians with polynomial-size gaps, while a shallow network through a restricted Boltzmann machine cannot efficiently represent those states unless the polynomial hierarchy in computational complexity theory collapses.

The Hilbert space dimension associated with quantum many-body problems is exponentially large, which poses a big challenge for solving those problems even with the most powerful computers. Variational approach is usually the tool of choice for tackling such difficult problems, which include many successful examples from simple mean-field approximation to more complicated methods such as those based on the matrix product states [1, 2], the tensor network states [3–6], the string bond states [7, 8], and more recently, the neural network states [6, 9]. The essence of the variational approach is to find an efficient representation of the relevant quantum many-body states. Here, by "efficient" we mean the number of parameters used to characterize those quantum states increases at most by a polynomial function with the number of particles (or degrees of freedom) in the system. With an efficient representation, one can then optimize those variational parameters by optimization techniques, such as the gradient descent method.

Neural network is a powerful tool to represent complex correlations in multiple-variable functions and recently finds wide applications in artificial intelligence through popularity of the deep learning methods [10]. An interesting connection has been made recently between the variational approach in quantum many-body problems and the learning method based on neural network representation [6]. Numerical evidence suggests that the restricted Boltzmann machine (RBM), a shallow generative neural network, optimized by the enforcement learning method, provides good solution to several many-body models [6]. Given this success, an important open question is what characterizes the representational power and limitation of the RBM for quantum many-body states.

In this paper, we characterize the representational power and limitation of the RBM and its extension to deep neural networks, the deep Boltzmann machine (DBM). We rigorously prove that a DBM can efficiently represent any quantum states generated by polynomial size quantum circuits or ground states of any k -local Hamiltonians with polynomial-size gaps. Here, " k -local" means that the Hamiltonian has only k -body interactions with a finite k (typically small) while the interaction range can be arbitrarily long; and "polynomial-size gap" means that the energy gap Δ approaches to zero at most by $1/\text{poly}(n)$, where $\text{poly}(n)$ denotes a polynomial function of the particle number n . Most physically relevant quantum states are either generated by many-body dynamics, which can be efficiently simulated through a polynomial size quantum circuit [11–13], or as ground states of some k -local Hamiltonians. So the DBM can efficiently represent most physical quantum states. We further prove that those classes of states cannot be efficiently represented by RBMs unless the polynomial hierarchy, a generalization of the famous P versus NP problem, collapses, which is believed to be highly unlikely in computer science. While having this limitation, the RBM can indeed represent many highly entangled states, and as examples we give explicit construction of their representation for arbitrary graph states [14], states with entanglement volume law or for critical systems [15], and topological toric code states [16].

Neural network quantum states. A many-body quantum state of n qubits can be written as $|\Psi\rangle = \sum_{\mathbf{v}} \Psi(\mathbf{v}) |\mathbf{v}\rangle$ in the computational basis with $\mathbf{v} \equiv (v_1, \dots, v_n)$, where the wave function $\Psi(\mathbf{v})$ is a general complex function of n binary variables $v_i \in \{0, 1\}$. In the neural network representation by a Boltzmann machine, the wave function $\Psi(\mathbf{v})$ is expressed as $\Psi(\mathbf{v}) = \sum_{\mathbf{h}} e^{W(\mathbf{v}, \mathbf{h})}$, where the weight $W(\mathbf{v}, \mathbf{h})$ is a complex quadratic function of binary variables \mathbf{v} and $\mathbf{h} \equiv (h_1, \dots, h_m)$ called visible and hidden neurons, respectively. The number of hidden neurons m is at most $\text{poly}(n)$ for an efficient representation. In the graphic representation shown in Fig. 1, the neurons v_i and h_j connected by an edge are correlated with a nonzero W_{ij} in the weight $W(\mathbf{v}, \mathbf{h}) = \sum_{i,j} W_{ij} v_i h_j$. For the RBM (Fig. 1a), the layer of visible neurons are connected to one layer of hidden neurons (neurons in the same layer are not mutually connected). The DBM is similar to the RBM but with two or more layers of hidden neurons (Fig. 1b). Two hidden layers are

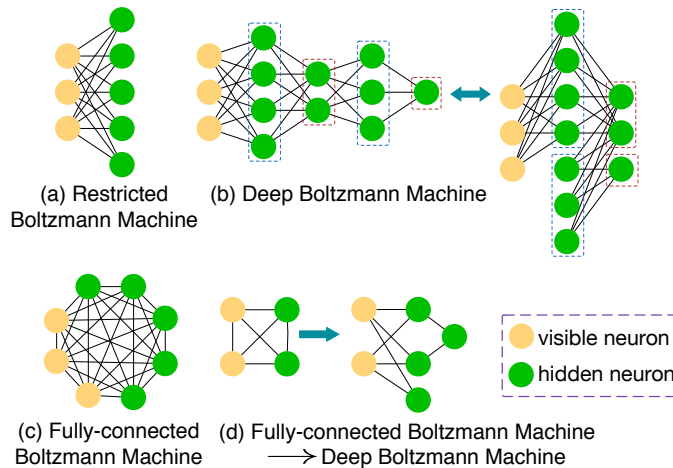


FIG. 1: **Illustration of Boltzmann machine neuron networks.** **a**, Restricted Boltzmann machine (RBM) which has only one hidden layer and no intra-layer connections. **b**, Deep Boltzmann machine (DBM) which has at least two hidden layers and no intra-layer connections. General DBMs are equivalent to DBMs with two hidden layers after rearrangement of odd and even layers. **c**, Fully-connected Boltzmann machine which has intra-layer connections. **d**, Reduction of fully-connected Boltzmann machine to DBMs with two hidden layers.

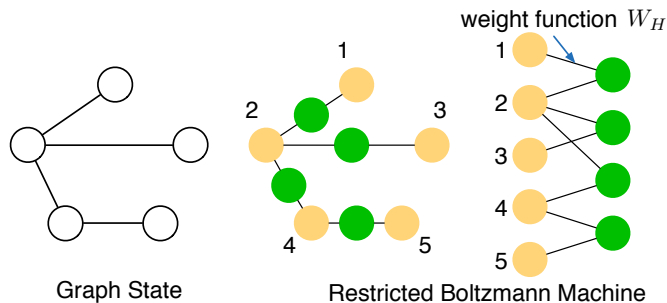


FIG. 2: **Representation of Graph states by RBMs.** One hidden neuron with the Hadamard weight function W_H (explicit form given in Eq. (1) of the text) simulates the correlation in the wave function between each pair of connected qubits in any graph states.

actually general enough as one can see in Fig. 1b that odd and even layers can each be combined into a single layer. A fully-connected Boltzmann machine is shown in Fig. 1c. In the methods section, we prove that any fully-connected Boltzmann machine can be efficiently represented by a DBM as illustrated in Fig. 1d.

Power and limitation of RBMs. RBMs can represent a wide class of many-body entangled states, including wave functions of any graph states [14], toric codes [16], and states violating the entanglement area law or for critical systems [15]. As an example, we give a simple construction for RBM representation of any graph states and leave the representation of other categories of states in the Supplementary Information. RBM representation for one-dimensional (1D) cluster states (a special case of graph states) and toric codes have been given recently in [9]. We give a different construction method which is significantly simpler and more systematic. The wave function of a graph state takes the form $\Psi(v_1, \dots, v_n) = \prod_{\langle i,j \rangle} (-1)^{v_i v_j} / \sqrt{2}$, where $\langle i,j \rangle$ denotes an edge linking the i -th and j -th qubits represented by visible neurons v_i, v_j . As shown in Fig. 2, one hidden neuron h and two edges with weight W_H realize the correlation function $(-1)^{v_i v_j} / \sqrt{2}$ between v_i and v_j . This requires to solve the equation $\sum_h e^{W_H(v_i, h) + W_H(v_j, h)} = (-1)^{v_i v_j} / \sqrt{2}$, which has a simple solution

$$W_H(x, h) = \frac{\pi}{8}i - \frac{\ln 2}{2} - \frac{\pi}{2}ix - \frac{\pi}{4}ih + i\pi xh \quad (1)$$

with $x = v_i$ or v_j .

The RBM state has an important property that its wave function $\Psi(\mathbf{v})$ can be calculated efficiently if a sample of \mathbf{v} is given (each v_i has been assigned a value). Here we prove that this property leads to limitation of the RBM to

represent more general quantum states. With a given sample of \mathbf{v} , $\Psi(\mathbf{v})$ can be factorized as

$$\prod_j \left(\prod_{i:(i,j)} e^{W_{ij}(v_i,0)} + \prod_{i:(i,j)} e^{W_{ij}(v_i,1)} \right) \quad (2)$$

where i (j) runs from 1 to at most n (m), so the total computational time for $\Psi(\mathbf{v})$ scales as mn for each sample of \mathbf{v} . This means $\Psi(\mathbf{v})$ can be computed by a circuit C_n with polynomial size $\text{poly}(n)$ for a given input $\mathbf{v} \in \{0, 1\}^n$. If a quantum state has a RBM representation (even if its explicit form is unknown), computing $\Psi(\mathbf{v})$ is characterized by the computational complexity class P/poly [17], which represent problems that can be solved by a polynomial size circuit even if the circuit cannot be constructed efficiently. The circuit here corresponds to a RBM representation, with the input given by a specific \mathbf{v} and the output given by the value of $\Psi(\mathbf{v})$.

We have introduced in Ref. [18] a specific quantum many-body state, denoted as Ψ_{GWD} , for which we proved it is $\#\text{P}$ -hard to calculate its wave function $\Psi_{\text{GWD}}(\mathbf{v})$ in the computational basis \mathbf{v} . If this state Ψ_{GWD} has a RBM representation, it means $\#\text{P} \subset \text{P/poly}$, an unlikely result in computational complexity theory as this means the polynomial hierarchy collapses [19, 20]. The state Ψ_{GWD} (with its explicit form given in the Supplementary Information) is just a 2D cluster state after a layer of translation-invariant single-qubit unitary operations. This state Ψ_{GWD} is (i) a universal quantum computational state that can be generated by a polynomial size quantum circuit; (ii) a projected entangled pair state (PEPS); (iii) the ground state of a gapped 5-local Hamiltonian. Combining the results above, we arrive at the following theorem:

Theorem 1 *RBM cannot efficiently represent universal quantum computational states, PEPS, and ground states of k -local Hamiltonians unless the polynomial hierarchy collapses.*

The above argument holds for exact representation of $\Psi(\mathbf{v})$ with RBM. Similar result holds even if we relax the requirement to have an approximate representation of $\Psi(\mathbf{v})$ with RBM, i.e., we require the trace distance between the targeted state and an optimal RBM state bounded by a small constant. As proved in detail in the Supplementary Information, under a reasonable complexity conjecture [18], the approximate RBM representation of the states listed in Theorem 1 still cannot be efficient if the polynomial hierarchy does not collapse.

Note that 2D cluster states can be efficiently represented by RBMs. While after a layer of single-qubit operations which do not change the quantum phase according to the classification scheme in Ref.[21, 22], the output state Ψ_{GWD} cannot be efficiently represented by RBMs any more. So RBM representation is not closed under unitaries that preserve a quantum phase.

Representational power of DBMs. Now we show with DBMs, i.e., with one more layer of hidden neurons, all the states listed in Theorem 1, which include most physical states, can be efficiently represented. For this purpose, first we introduce a couple of gadgets that will simplify our construction.

Gadget is a complex function of binary variables after encapsulation of hidden neurons in a DBM network as shown in Fig. 3(a), where the input is represented by port neurons (for connection of different gadgets) and the output is the value of the function. We use gadgets as basic elements in a large DBM. As examples, we define Hadamard gadget and phase gadget as shown in Fig. 3(b), which will play the role of elementary gates for construction of DBM representation of quantum circuits. The weight function W_H is given by Eq. (1) and W_θ is the solution of the equation $\sum_h e^{W_\theta(x_1,h)+W_\theta(x_2,h)} = e^{i\theta x_1} \delta_{x_1 x_2}$, which may take the form

$$W_\theta(x, h) = -\frac{\ln 2}{2} + \frac{\theta}{2}ix + i\pi xh. \quad (3)$$

We can combine two gadgets g_1, g_2 into one gadget g by two types of fusion rules shown in Fig. 3(c):

$$\text{rule I: } g(\cdot, \cdot) = \sum_x g_1(\cdot, x)g_2(x, \cdot), \quad (4)$$

$$\text{rule II: } g(\cdot, x, \cdot) = g_1(\cdot, x)g_2(x, \cdot), \quad (5)$$

where rule I simulates matrix multiplication.

With these tools, now we construct efficient DBM representation of any quantum states generated by a polynomial size circuit. The Hadamard gadget and phase gadget as shown in Fig. 3(b) are used to construct three elementary quantum gates: Hadamard gate H , phase gate $Z(\theta)$ with an arbitrary phase θ , and controlled phase flip gate CZ , which together are universal for quantum computation [23, 24]. The initial state of the circuit is taken as $(|0\rangle + |1\rangle)^{\otimes n}$, an equal superposition of computational basis states, which is represented by the wave function $\phi_0(x_1, \dots, x_n) = 1$,

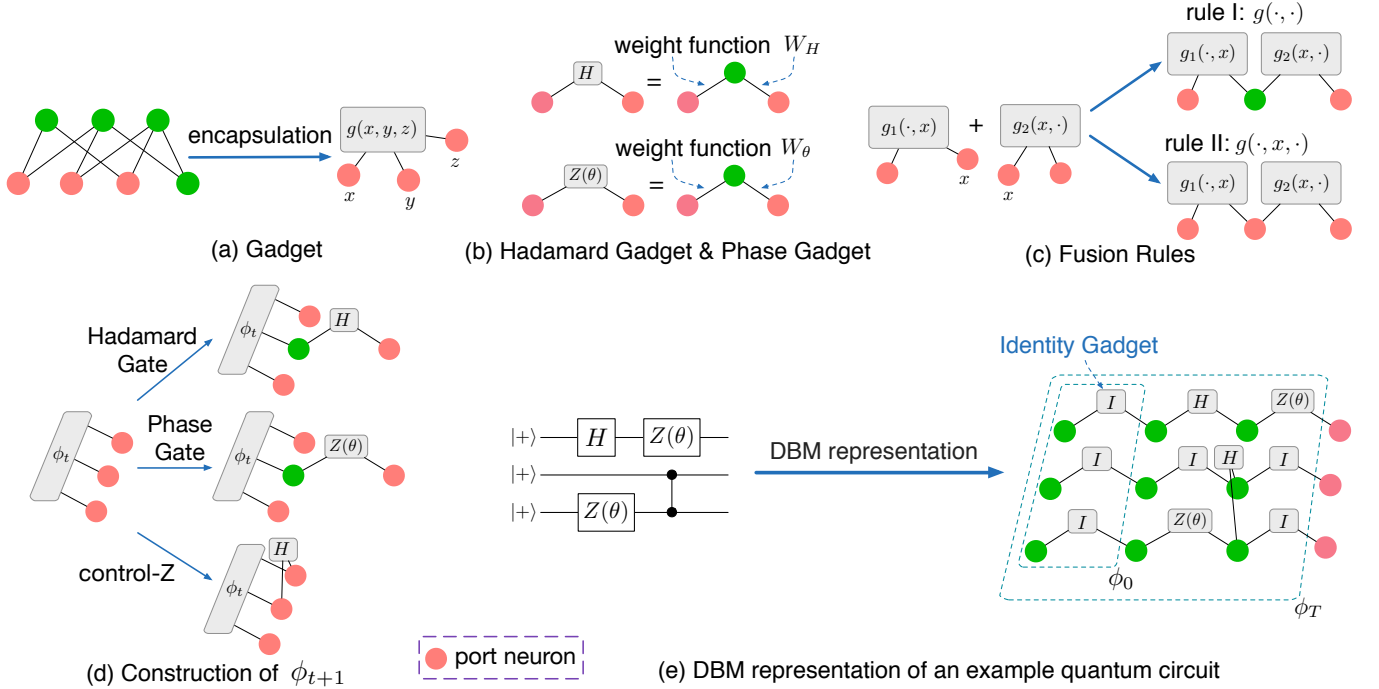


FIG. 3: **Representation of universal quantum computational states by DBMs.** **a**, Gadget is a complex function of binary variables represented by port neurons, a short-hand notation after encapsulation of hidden neurons. **b**, Two elementary gadgets for representation of quantum circuits: Hadamard gadget with weight W_H given by Eq. (1) and phase gadget with weight W_θ given by Eq. (3). **c**, Two types of fusion rules for gadgets: rule I and rule II and their neuron network representation. **d**, Fusion with phase or Hadamard gadgets with rule I or rule II simulates application of three elementary quantum gates: the phase gate, the Hadamard gate, and the controlled phase flip gate, which together make universal quantum computation. The figure illustrates evolution of the wave function from step t to step $t + 1$. **e**, Representation of an example quantum circuits with elementary gadgets. To represent circuits of depths T , we need to apply T steps of fusions with elementary gadgets, and gadget fusions in the same step can be applied in parallel. The identity gadget is a special phase gadget with $\theta = 0$. After the last (T) step of computation, port neurons become visible neurons to represent the index of physical qubits, and we get a DBM representation of the output state.

the identity gadget. Denote the wave function after applying t -layer of elementary gates as $\phi_t(x_1, \dots, x_n)$. As shown in Fig. 3(d), using rule I (corresponding to matrix multiplication), Hadamard gadget and phase gadget simulate gates H and $Z(\theta)$. Using rule II with Hadamard gadget, we have

$$\phi_{t+1}(\dots x_i, x_{i+1} \dots) = (-1)^{x_i x_{i+1}} \phi_t(\dots x_i, x_{i+1}, \dots) / \sqrt{2}, \quad (6)$$

which simulates the CZ gate except for the unimportant normalization factor $1/\sqrt{2}$. The above procedure can be paralleled as illustrated in Fig. 3(e), which shows the DBM representation of an example circuit. For a quantum circuit of depth T , we apply T steps of fusion rules, and each step needs $O(n)$ neurons. So the DBM representation of the output state of the quantum circuit takes $O(nT)$ neurons. This DBM representation is sparse, meaning that each neuron has a constant coordination number (number of connected edges) that does not increase with the size of neuron network. We therefore have the following theorem:

Theorem 2 *Any quantum state of n qubits generated by a quantum circuit of depth T can be represented exactly by a sparse DBM with $O(nT)$ neurons.*

Using the above theorem, we now construct efficient DBM representation of any tensor network states, which include the PEPS and the MERA states as special cases [4, 25, 26]. Suppose the local tensor is $A_{b_1 \dots b_d p}$, which has one (or zero) physical index p and d bond indices b_1, \dots, b_d , each ranging from 1 to the bond dimension D . Without loss of generality, we assume p is binary and $D = 2^k$ for some integer k and write the local tensor as a function $A_{x_1 \dots x_c}$, where each x_i is a binary variable and $c = kd + 1$. The state of $|A\rangle = \sum_{x_1, \dots, x_c} A_{x_1 \dots x_c} |x_1, \dots, x_c\rangle$ can be generated by a quantum circuit with the number of elementary gates on the order of $O(2^{2(kd+1)}) = O(D^{2d})$ [24], which is square

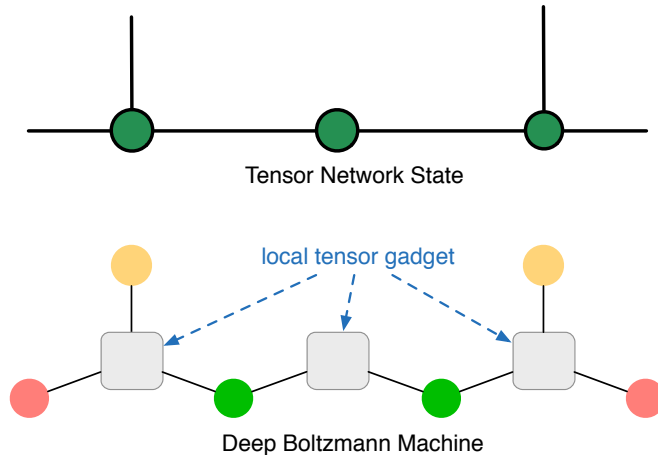


FIG. 4: **Representation of tensor network states with DBMs.** Visible (hidden) neurons play the role of physical (bond) indices, respectively. Port neuron represents either the bond index for the next step of tensor contraction or the physical index if there is no further contraction. The grey box stands for the local tensor gadget $A_{x_1 \dots x_c}$ which can be efficiently represented with a DBM.

of the Hilbert space dimension of $\text{span}(|x_1, \dots, x_c\rangle)$. Using Theorem 2, the state $|A\rangle$ can be represented by a DBM with $O(D^{2d})$ neurons, and the resultant representation is called the local tensor gadget. We use fusion rule I to link two local tensor gadgets to simulate contraction of bond index and put physical index in the visible layer, as shown in Fig. 4. We thus have the following theorem:

Theorem 3 *Tensor network state with bond dimension D , maximum coordination number d , and n local tensors, can be represented efficiently by a sparse DBM with $O(nD^{2d})$ neurons.*

Tensor network state can represent ground state of a Hamiltonian by simulating imaginary time evolution through Trotter decomposition [27–29]. Recently, quantum simulation based on truncated Taylor series has been proposed [13] which has exponential improvement on precision compared to traditional methods based on Trotter decomposition. Inspired by this idea, we construct tensor network simulation for imaginary time evolution of any k -local Hamiltonian based on truncated Taylor series. Compared to previous method [27], our construction offers exponential improvement on precision. The detailed proof is included in the Supplementary Information. Combining with theorem 3, we then construct an efficient DBM representation of ground state of any k -local Hamiltonian, described by the following theorem:

Theorem 4 *The ground state of any k -local Hamiltonian can be represented by a sparse DBM with neuron number*

$$O\left(\frac{1}{\Delta} \left(n + \log \frac{1}{\epsilon}\right) m^2\right), \quad (7)$$

where n is the particle number, m is number of interaction terms in the Hamiltonian, Δ is the energy gap, and ϵ is the representational error in terms of trace distance.

This representation is efficient as long as the energy gap Δ vanishes with increase of n no faster than $1/\text{poly}(n)$, which is typically true for physical Hamiltonians (even if they are gapless in the thermodynamic limit).

Discussion. With popularity and success of the deep learning methods, a question often raised is why depth of a neural network is so important [10]. Our proof of the exponential gap in efficiency of using the DBMs and the RBMs to represent quantum many-body states helps to address this fundamentally important question in a new context of solving problems in the quantum world. We have proven that most physical quantum states, either from quantum dynamics or as ground states of complicated Hamiltonians, can be efficiently represented by DBMs. This result is of fundamental interest and may open up an exciting prospect of using deep learning methods through neural network representation to tackle strongly correlated many-body problems, a challenging frontier of modern physics.

METHODS

Here we prove that any fully-connected Boltzmann machine (with intra-layer edges) can be efficiently simulated with DBMs (without intra-layer connections) as shown in Fig. 1(d). The key point is to simulate the interaction between two neurons by a gadget $\sum_h e^{W_1(x_1,h)+W_2(x_2,h)} = e^{W_0(x_1,x_2)}$. Suppose the interaction term is Jx_1x_2 in W_0 , we need $W_1 + W_2 = a - \ln 2 + b(x_1 + x_2)(2h - 1) + c(2h - 1) + d(x_1 + x_2)$ to simulate the interaction with the aid of hidden neuron h , where the parameters a, b, c, d need to satisfy the equations $e^a \cosh(c) = 1$, $e^a e^d \cosh(b + c) = 1$, $e^a e^{2d} \cosh(2b + c) = e^J$. These equations have solutions, one of them is

$$a = -d = -J/2, b = -c = -i \arccos(e^{J/2}). \quad (8)$$

-
- [1] Schollwöck, U. The density-matrix renormalization group. *Reviews of modern physics* **77**, 259 (2005).
 - [2] Schollwöck, U. The density-matrix renormalization group in the age of matrix product states. *Annals of Physics* **326**, 96–192 (2011).
 - [3] Verstraete, F., Murg, V. & Cirac, J. I. Matrix product states, projected entangled pair states, and variational renormalization group methods for quantum spin systems. *Advances in Physics* **57**, 143–224 (2008).
 - [4] Vidal, G. Entanglement renormalization. *Physical review letters* **99**, 220405 (2007).
 - [5] Orús, R. A practical introduction to tensor networks: Matrix product states and projected entangled pair states. *Annals of Physics* **349**, 117–158 (2014).
 - [6] Carleo, G. & Troyer, M. Solving the quantum many-body problem with artificial neural networks. *arXiv preprint arXiv:1606.02318* (2016).
 - [7] Schuch, N., Wolf, M. M., Verstraete, F. & Cirac, J. I. Simulation of quantum many-body systems with strings of operators and monte carlo tensor contractions. *Physical review letters* **100**, 040501 (2008).
 - [8] Sfondrini, A., Cerrillo, J., Schuch, N. & Cirac, J. I. Simulating two- and three-dimensional frustrated quantum systems with string-bond states. *Physical Review B* **81**, 214426 (2010).
 - [9] Deng, D.-L., Li, X. & Sarma, S. D. Exact machine learning topological states. *arXiv preprint arXiv:1609.09060* (2016).
 - [10] LeCun, Y., Bengio, Y. & Hinton, G. Deep learning. *Nature* **521**, 436–444 (2015).
 - [11] Lloyd, S. Universal quantum simulators. *Science* **273**, 1073 (1996).
 - [12] Poulin, D., Qarry, A., Somma, R. & Verstraete, F. Quantum simulation of time-dependent hamiltonians and the convenient illusion of hilbert space. *Physical review letters* **106**, 170501 (2011).
 - [13] Berry, D. W., Childs, A. M., Cleve, R., Kothari, R. & Somma, R. D. Simulating hamiltonian dynamics with a truncated taylor series. *Physical review letters* **114**, 090502 (2015).
 - [14] Raussendorf, R. & Briegel, H. J. A one-way quantum computer. *Physical Review Letters* **86**, 5188 (2001).
 - [15] Verstraete, F., Wolf, M. M., Perez-Garcia, D. & Cirac, J. I. Criticality, the area law, and the computational power of projected entangled pair states. *Physical review letters* **96**, 220601 (2006).
 - [16] Kitaev, A. Y. Fault-tolerant quantum computation by anyons. *Annals of Physics* **303**, 2–30 (2003).
 - [17] Arora, S. & Barak, B. *Computational complexity: a modern approach* (Cambridge University Press, 2009).
 - [18] Gao, X., Wang, S.-T. & Duan, L.-M. Quantum supremacy for simulating a translation-invariant ising spin model. *arXiv preprint arXiv:1607.04947* (2016).
 - [19] Karp, R. M. & Lipton, R. Turing machines that take advice. *Enseign. Math* **28**, 191–209 (1982).
 - [20] Babai, L., Fortnow, L. & Lund, C. Nondeterministic exponential time has two-prover interactive protocols. In *Foundations of Computer Science, 1990. Proceedings., 31st Annual Symposium on*, 16–25 (IEEE, 1990).
 - [21] Hastings, M. B. & Wen, X.-G. Quasiadiabatic continuation of quantum states: The stability of topological ground-state degeneracy and emergent gauge invariance. *Physical review b* **72**, 045141 (2005).
 - [22] Chen, X., Gu, Z.-C. & Wen, X.-G. Local unitary transformation, long-range quantum entanglement, wave function renormalization, and topological order. *Physical review b* **82**, 155138 (2010).
 - [23] Barenco, A. *et al.* Elementary gates for quantum computation. *Physical review A* **52**, 3457 (1995).
 - [24] Nielsen, M. A. & Chuang, I. L. *Quantum computation and quantum information* (Cambridge university press, 2010).
 - [25] Verstraete, F. & Cirac, J. I. Renormalization algorithms for quantum-many body systems in two and higher dimensions. *arXiv preprint cond-mat/0407066* (2004).
 - [26] Bridgeman, J. C. & Chubb, C. T. Hand-waving and interpretive dance: An introductory course on tensor networks. *arXiv preprint arXiv:1603.03039* (2016).
 - [27] Schuch, N., Wolf, M. M., Verstraete, F. & Cirac, J. I. Computational complexity of projected entangled pair states. *Physical review letters* **98**, 140506 (2007).
 - [28] Vidal, G. Efficient classical simulation of slightly entangled quantum computations. *Physical Review Letters* **91**, 147902 (2003).
 - [29] Orus, R. & Vidal, G. Infinite time-evolving block decimation algorithm beyond unitary evolution. *Physical Review B* **78**, 155117 (2008).

- [30] Vitagliano, G., Riera, A. & Latorre, J. Volume-law scaling for the entanglement entropy in spin-1/2 chains. *New Journal of Physics* **12**, 113049 (2010).
- [31] Gu, Z.-C., Levin, M., Swingle, B. & Wen, X.-G. Tensor-product representations for string-net condensed states. *Physical Review B* **79**, 085118 (2009).
- [32] Broadbent, A., Fitzsimons, J. & Kashefi, E. Universal blind quantum computation. In *Foundations of Computer Science, 2009. FOCSS'09. 50th Annual IEEE Symposium on*, 517–526 (IEEE, 2009).
- [33] Boixo, S. *et al.* Characterizing quantum supremacy in near-term devices. *arXiv preprint arXiv:1608.00263* (2016).

Acknowledgements We thank Ignacio Cirac and Sheng-Tao Wang for helpful discussions. This work was supported by the Ministry of Education of China and Tsinghua University. LMD acknowledges in addition support from the AFOSR MURI program.

Author Information All the authors contribute substantially to this work. Correspondence and requests for materials should be addressed to L.M.D. (lmduan@umich.edu) or X. G. (gaoxungx@gmail.com).

SUPPLEMENTARY INFORMATION

In this Supplementary Information, we provide details on derivations and proofs in main text, including, (i) a detailed derivation of the weight functions W_H and W_θ ; (ii) construction of RBM representation for toric codes and for states with entanglement volume law or critical behaviors. (iii) a proof of theorem 1 for limitation of RBM in the case of approximate representation; (iv) a proof of theorem 4 for DBM representation of ground states of any k -local Hamiltonians.

Detailed derivation of the weight functions W_H and W_θ

In main text, we give the expression for W_H and W_θ which can be obtained by setting a general form for them as $a + bx + ch + dxh$ and solving the resultant equations for the parameters a, b, c, d . Here, we give the detailed derivation.

For the Hadamard gadget which is used to construct RBM representation for graph states and simulate H and CZ gates, the equation we need to solve is

$$\sum_{h=0,1} e^{W_H(x_1,h)+W_H(x_2,h)} = H_{x_1x_2} \quad (9)$$

where the correlation

$$H_{x_1x_2} = \frac{(-1)^{x_1x_2}}{\sqrt{2}} = \cos\left(\frac{\pi}{4}[2(x_1+x_2)-1]\right). \quad (10)$$

The last step in Eq.(2) is valid since we have $H_{x_1x_2} = 1/\sqrt{2}, 1/\sqrt{2}, -1/\sqrt{2}$ when $x_1+x_2 = 0, 1, 2$, respectively. Using the relation

$$\cos X = \frac{e^{iX} + e^{-iX}}{2} = \sum_h e^{iX(2h-1)-\ln 2}. \quad (11)$$

with $X = \pi/4[2(x_1+x_2)-1]$, we get

$$W_H(x_i, h) = i\pi x_i h - i\pi[2x_i + h]/4 + (i\pi/4 - \ln 2)/2.$$

for $x_i = x_1$ or x_2 .

For the Phase gadget which is used to simulate $Z(\theta)$ gate, we need to satisfy

$$\sum_{h=0,1} e^{W_\theta(x_1,h)+W_\theta(x_2,h)} = Z(\theta)_{x_1x_2} = \delta_{x_1x_2} e^{i\theta x_1} \quad (12)$$

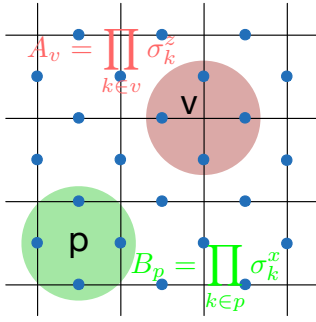
We simulate $\delta_{x_1x_2}$ by the following observation

$$\delta_{x_1x_2} = \frac{1 + e^{i\pi(x_1+x_2)}}{2} = \sum_h e^{i\pi(x_1+x_2)h - \ln 2}. \quad (13)$$

Note that $\delta_{x_1x_2} e^{i\theta x_1} = \delta_{x_1x_2} e^{i\theta(x_1+x_2)/2}$, we have the solution

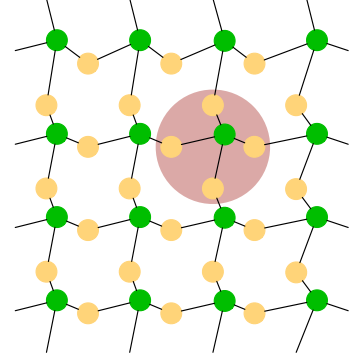
$$W_\theta(x_i, h) = i\pi x_i h + (i\theta x_i - \ln 2)/2. \quad (14)$$

(a) Toric code

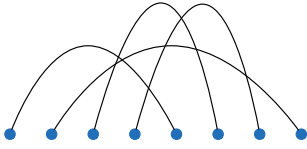


$$v = \begin{cases} 1, & v_1 + v_2 + v_3 + v_4 \text{ even} \\ 0, & v_1 + v_2 + v_3 + v_4 \text{ odd} \end{cases}$$

$$W(v, h) = i\pi v h - (\ln 2)/4$$

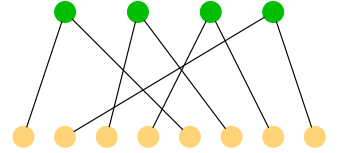


(b) Random Entanglement Pair

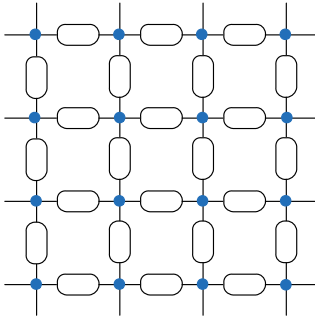


$$v_1 v_2 = \delta_{v_1 v_2}$$

$$W(v, h) = i\pi v h - (\ln 2)/2$$



(c) Coherent thermal state



$$v_1 v_2 = e^{-\beta v_1 v_2 / 2}$$

$$W(v, h) = a/2 - (\ln 2)/2 + bv(2h - 1) + c(2h - 1)/2 + dv$$

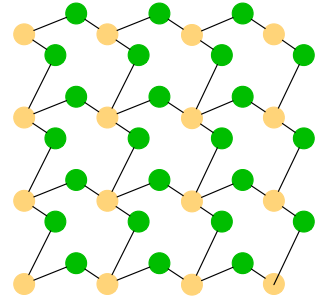


FIG. 5: RBM representation (shown on the right side) of some many-body entangled states (defined on the left side). (a) Toric code is the simplest topologically ordered state and is used as a quantum error correcting code. The wave function for the toric code is a product of functions shown in the figure for each vertex v . (b) Randomly distributed Entangled pairs $|00\rangle + |11\rangle$ on a line (or any lattice). The state obeys the entanglement volume law. The wave function of this state is a simple product of functions shown in the figure for each pair. (c) Coherent thermal state which represents a critical system when β reaches β_c , the critical point in the corresponding thermal state of the classical Ising model. The wave function is square root of the corresponding probability in classical thermal model. For RBM representation, the coefficient a, b, c, d is given by the solution in the method section of the main text with J replaced by $-\beta/2$.

RBM representation of many-body entangled states

In this construction, we restrict to simple RBM gadget with only one hidden neuron connected to k visible neurons and identical weight function W on each edge. we need to solve the equation

$$\sum_h e^{W(v_1, h) + \dots + W(v_k, h)} = g(v_1, \dots, v_k) \quad (15)$$

for a certain correlation $g(v_1, \dots, v_k)$. Apart from the graph state example given in the main text, we construct RBM representation of three classes of entangled states: the toric code, which is the simplest state with topological order and useful for quantum error correction; the randomly distributed entangled pair state, which satisfies the entanglement volume law instead of the area law [30]; and the coherent thermal state which describes a critical system [15]. These examples and the corresponding RBM representations are shown in Fig. 5.

For the toric code, the correlation function $g(v_1, v_2, v_3, v_4) = (v_1 + v_2 + v_3 + v_4 \pmod 2)$ on each vertex and the wave function is a product of these functions over all vertices [31]. We have

$$g(v_1, v_2, v_3, v_4) = \frac{1 + e^{i\pi(v_1+v_2+v_3+v_4)}}{2} = \sum_{h=0,1} e^{i\pi(v_1+v_2+v_3+v_4)h - \ln 2}, \quad (16)$$

so the weight $W(v_i, h) = i\pi v_i h - (\ln 2)/4$ for the toric code example. Ref. [9] gives another construction of RBM representation of the toric code state, and compared with that our construction here is significantly simpler.

For the randomly distributed entangled pair states, we have $g(v_1, v_2) = \delta_{v_1 v_2}$ for each entangled pair $|00\rangle + |11\rangle$. The weight function $W(v_i, h)$ is a special case of the phase gadget W_θ with $\theta = 0$ (the identity gadget).

For a coherent thermal state defined as

$$|\Psi_{ch}\rangle = \sum_{\mathbf{v}} \prod_{\langle i,j \rangle} e^{-\beta v_i v_j / 2} |\mathbf{v}\rangle, \quad (17)$$

it has the same correlation function as the corresponding thermal state with β denoting the inverse temperature [15]. We consider the binary variables \mathbf{v} defined on a square lattice as shown in Fig. 5, and the state $|\Psi_{ch}\rangle$ then defines a coherent thermal state for a 2D Ising model which has a phase transition at $\beta = \beta_c$. At this critical point β_c , the state $|\Psi_{ch}\rangle$ describes a many-body entangled state for a critical system. For any value of β , the wave function of the state $|\Psi_{ch}\rangle$ can be simply represented by a RBM as shown in Fig. 5. We have $g(v_1, v_2) = e^{-\beta v_1 v_2 / 2}$ for each pair of visible neurons. The correlation is identical to the case that we have considered for the DBM representation of a fully connect Boltzmann machine (see the method section of the main text). We just need a single hidden neuron to generate this correlation with the weight function given in the method section of the main text where J is replaced by $-\beta/2$.

Proof of theorem 1 under approximation representation

Here we introduce a specific state on 2D lattice, denoted as $|\psi_{\text{GWD}}\rangle$ and shown in Fig. 6. State $|\psi_{\text{GWD}}\rangle$ is cluster state after one layer translation-invariant single-qubit unitary transformation. This state was introduced in Ref. [18] for proof of quantum supremacy. We prove here $|\psi_{\text{GWD}}\rangle$ cannot be efficiently represented by RBMs under reasonable conjectures in complexity theory. This no-go theorem holds for both exact and approximate representation.

Exact representation

Suppose the coefficient of $|\psi_{\text{GWD}}\rangle$ in the computational basis is $\Psi(\mathbf{v})$ (In term of notation, $|\Psi(\mathbf{v})|^2$ corresponds to q_x in Ref. [18]). In Ref. [18], it is proved that computing $|\Psi(\mathbf{v})|^2$ is $\#\text{P}$ -hard where $|\tilde{\Psi}(\mathbf{v})|^2$ is an estimation of $|\Psi(\mathbf{v})|^2$ such that

$$\left| |\Psi(\mathbf{v})|^2 - |\tilde{\Psi}(\mathbf{v})|^2 \right| \leq \frac{|\Psi(\mathbf{v})|^2}{\text{poly}(n)} + \frac{c}{2^{mn}} \quad (18)$$

where $0 \leq c < 1/2$ and the lattice size is $n \times m$. This equation implies computing $|\tilde{\Psi}(\mathbf{v})|^2$ is also $\#\text{P}$ -hard such that

$$\left| |\Psi(\mathbf{v})|^2 - |\tilde{\Psi}(\mathbf{v})|^2 \right| \leq \frac{c}{2^{mn}}. \quad (19)$$

Denote \mathcal{O} as an oracle with the ability to compute the first $mn - 1$ digits of $\Psi(\mathbf{v})$. The above statement implies

$$\mathbf{P}^{\#\text{P}} \subseteq \mathbf{P}^{\mathcal{O}}. \quad (20)$$

If $|\psi_{\text{GWD}}\rangle$ can be represented efficiently by a RBM, calculating its wave function in the computational basis belongs to the complexity class \mathbf{P}/poly as discussed in the main text. Thus $\mathcal{O} \subseteq \mathbf{P}/\text{poly}$. Combining these results, we have

Lemma 1 *RBM cannot represent $|\psi_{\text{GWD}}\rangle$ exactly unless*

$$\mathbf{P}^{\#\text{P}} \subseteq \mathbf{P}^{\mathbf{P}/\text{poly}}. \quad (21)$$

Ref. [20] proves if the containment in the above equation is true, the polynomial hierarchy will collapse [17], which is widely believed to be unlikely.

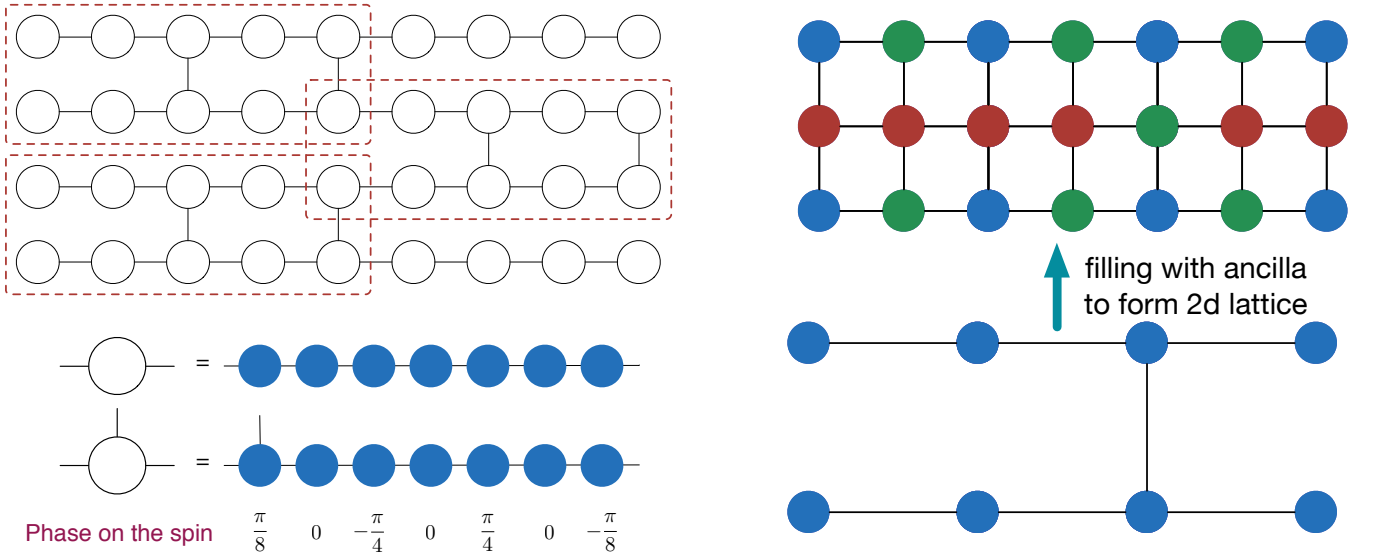


FIG. 6: The state $|\psi_{\text{GWD}}\rangle$ used in the proof of theorem 1, which is introduced in Ref. [18] for proof of quantum Supremacy. To construct this state, we start from a brickwork of white circles [32] (the left top side), with each white circle represented by seven blue circles. Each blue circle represents a qubit, and the brickwork of blue circles can be filled with additional red and green circles (each represent an ancillary qubit) to form a regular 2D square lattice (shown on the right top side). We start with a standard 2D cluster state for the square lattice, and then apply the phase gates $Z(\theta)$ on the blue-circle qubits with the angle θ forming a periodic pattern shown in the left bottom figure and the Hadamard gate on each green-circle and blue-circle qubits (no gate on the red-circle qubits). After this layer of single-qubit unitary operations, we get the state $|\psi_{\text{GWD}}\rangle$.

Approximate representation

Denote a measurement in the computational basis as a quantum operator \mathcal{E} and $\tilde{\Psi}(\mathbf{v})$ as the wave function of a RBM state $|\psi'_{\text{GWD}}\rangle$ to approximate $|\psi_{\text{GWD}}\rangle$, then we have

$$\sum_{\mathbf{v}} \left| |\Psi(\mathbf{v})|^2 - |\tilde{\Psi}(\mathbf{v})|^2 \right| = 2D(\mathcal{E}(|\psi_{\text{GWD}}\rangle\langle\psi_{\text{GWD}}|), \mathcal{E}(|\psi'_{\text{GWD}}\rangle\langle\psi'_{\text{GWD}}|)) \leq 2D(|\psi_{\text{GWD}}\rangle\langle\psi_{\text{GWD}}|, |\psi'_{\text{GWD}}\rangle\langle\psi'_{\text{GWD}}|) \leq \epsilon, \quad (22)$$

where $D(\rho_1, \rho_2)$ denotes the trace distance, defined as $\text{tr}|\rho_1 - \rho_2|/2$. The above equation means if the trace distance between $|\psi_{\text{GWD}}\rangle$ and $|\psi'_{\text{GWD}}\rangle$ is smaller than $\epsilon/2$, we have $\mathbb{E}_{\mathbf{v}} \left[\left| |\Psi(\mathbf{v})|^2 - |\tilde{\Psi}(\mathbf{v})|^2 \right| \right] \leq \epsilon/2^{mn}$ where $\mathbb{E}_{\mathbf{v}}[f(\mathbf{v})]$ means the expectation value of $f(\mathbf{v})$ over uniform distribution of \mathbf{v} . Using the Markov inequality, we get

$$\Pr_{\mathbf{v}} \left[\left| |\Psi(\mathbf{v})|^2 - |\tilde{\Psi}(\mathbf{v})|^2 \right| \geq \frac{\epsilon}{2^{mn}\delta} \right] \leq \delta, \quad (23)$$

where $\epsilon/\delta < 1/2$ and $\Pr_{\mathbf{v}}[f(\mathbf{v})]$ denotes the probability such that \mathbf{v} satisfies condition $f(\mathbf{v})$ if random variable \mathbf{v} is uniform distributed. This equation means that for $1 - \delta$ fraction of the whole set \mathbf{v} , we have

$$\left| |\Psi(\mathbf{v})|^2 - |\tilde{\Psi}(\mathbf{v})|^2 \right| \leq \frac{\epsilon}{2^{mn}\delta}. \quad (24)$$

Denote \mathcal{O}' as an oracle with the ability to compute the first $mn - 1$ digits of $|\Psi(\mathbf{v})|^2$ for such fraction of \mathbf{v} , then $\mathcal{O}' \subseteq \mathcal{O} \subseteq \text{P/poly}$.

In Ref. [18], we introduced a conjecture that #P-hardness of approximating $\Psi(\mathbf{v})$ to the error given by Eq. (24) still holds when we lift from the worst-case to the average-case, that is,

Conjecture 1 For any $1 - \delta$ fraction of instance \mathbf{v} , approximating $|\Psi(\mathbf{v})|^2$ by $|\tilde{\Psi}(\mathbf{v})|^2$ up to the error

$$\left| |\Psi(\mathbf{v})|^2 - |\tilde{\Psi}(\mathbf{v})|^2 \right| \leq \frac{\epsilon}{2^{mn}\delta}$$

is still #P-hard.

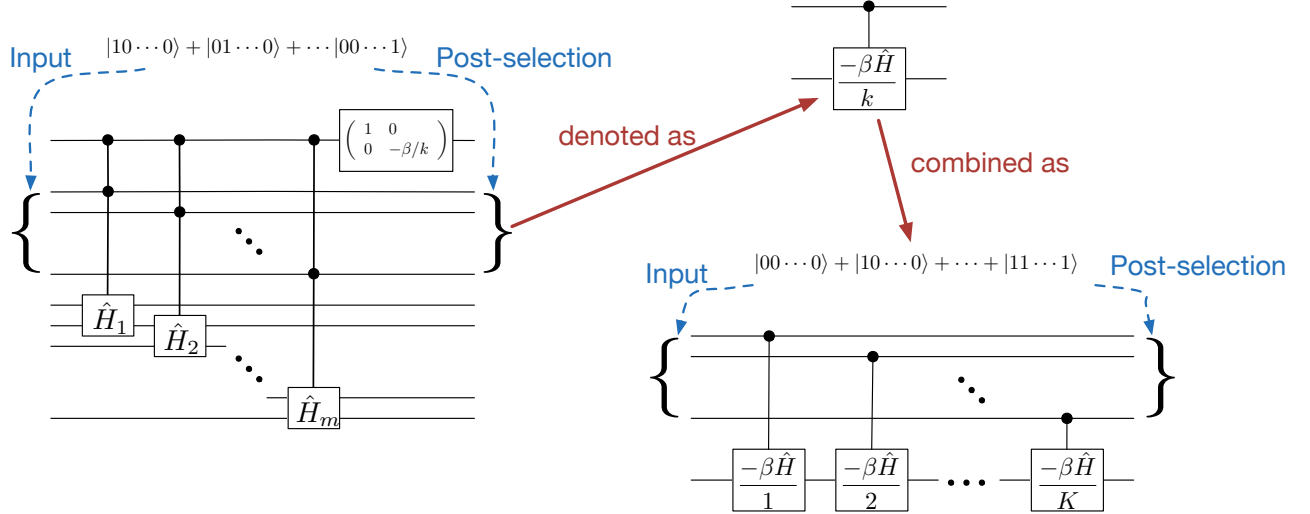


FIG. 7: Construction of pseudo quantum circuit where each elementary gate represents a linear but non-unitary operation which can be described through multiplication of a local tensor. The left diagram represents construction of the pseudo-gate controlled- $(-\beta\hat{H}/k)$, which acts as a basic building block for construction of the pseudo-gate $e^{-\beta\hat{H}}$ shown on the lower right side through the Taylor series expansion.

Ref. [18] has discussed why this is a reasonable conjecture. It is related to classical-hardness for simulating distribution from random quantum circuit and is supported by both quantum chaos theory and extensive numerical simulations [33]. With this conjecture, we have

$$\mathbf{P}^{\#P} \subseteq \mathbf{P}^{O'}. \quad (25)$$

Combining the results above, we have the following theorem

Lemma 2 *If the conjecture 1 is true, any RBM states cannot approximate $|\psi_{\text{GWD}}\rangle$ with the trace distance smaller than $\epsilon/2$, otherwise $\mathbf{P}^{\#P} \subseteq \mathbf{P}^{\text{P/poly}}$ and the polynomial hierarchy collapses.*

Efficient tensor network representation for ground states

In proof of theorem 4, we mention that we have developed a method using Taylor series expansion to efficiently construct ground states of any k -local Hamiltonians with tensor network (and thus DBM network as well due to theorem 3). Compared with the previous construction method [27], this approach allows an exponential improvement in the precision of the representation. We use pseudo quantum circuit to present our construction as shown in Fig. 7. Pseudo quantum circuit is similar to conventional quantum circuit except that the pseudo-gate is not required to be unitary. Each pseudo-gate still represents a linear transformation through matrix multiplication, so it can be easily constructed through a local tensor. The pseudo quantum circuit then just represents a tensor network.

Suppose the number of interaction terms in the Hamiltonian is m , i.e., $\hat{H} \equiv \sum_{i=1}^m \hat{H}_i$, where each \hat{H}_i involves at most k -body interactions (k is typically a small finite constant). We simulate the operator \hat{H} by first generating a state $\sum_{i=1}^m |i\rangle$, where $|i\rangle \equiv |0_1 0_2 \dots 1_i \dots 0_m\rangle$, i.e., only the i -th bit is 1. Applying the operation \hat{H}_i controlled by the i -th qubit as shown in Fig. 7 and post-selecting the control bits in the state $\sum_{i=1}^m |i\rangle$ (note that postselection can be easily represented in a tensor network), we get

$$\sum_{i=1}^m |i\rangle \xrightarrow{\text{controlled-}\hat{H}_i} \sum_{i=1}^m |i\rangle \hat{H}_i \xrightarrow{\text{post-selection}} \sum_{i=1}^m \hat{H}_i. \quad (26)$$

This requires $O(m)$ pseudo quantum gates as shown in Fig. 7. All of the above operations are controlled by an additional qubit (see Fig. 7). We then apply a non-unitary matrix $\text{diag}(1, -\beta/k)$ on this control qubit, and construct a pseudo-gate controlled- $(-\beta\hat{H}/k)$. Note that this gate requires $O(m)$ elementary pseudo quantum gates for its

construction and we use the pseudo-gate controlled- $(-\beta\hat{H}/k)$ as a building block for the next step. In the next step, we first generate a superposition state $\sum_{k=0}^K |k\rangle$, where K corresponds to the truncation number in Taylor series expansion and $|k\rangle \equiv |1_1 1_2 \cdots 1_k 0_{k+1} \cdots 0_K\rangle$, i.e. only the first k bits are in state $|1\rangle$. Applying the circuit shown in Fig. 7 and post-selecting the output state of the control qubits in $\sum_{k=0}^K |k\rangle$, we get

$$\sum_{k=0}^K |k\rangle \xrightarrow{\text{controlled-}(-\beta\hat{H}/k)} \sum_{k=0}^K |k\rangle \frac{(-\beta\hat{H})^k}{k!} \xrightarrow{\text{post-selection}} \sum_{k=0}^K \frac{(-\beta\hat{H})^k}{k!} \quad (27)$$

which is the Taylor expansion of $e^{-\beta\hat{H}}$ truncated to the K -th order. Note that this construction of $e^{-\beta\hat{H}}$ requires $O(Km)$ elementary pseudo quantum gates.

We apply the above operator $e^{-\beta\hat{H}}$ on the state

$$\sum_{i=0}^{2^n-1} |i\rangle|i\rangle = \sum_{i=0}^{2^n-1} |\psi_i\rangle|\psi_i^*\rangle \quad (28)$$

where n represents the total number of qubits in the Hamiltonian \hat{H} , $|\psi_i\rangle$ denotes the i -th eigenstate of \hat{H} , and $|\psi_i^*\rangle$ is the complex conjugate of $|\psi_i\rangle$ in the computational basis. After tracing out the register storing $|\psi_i^*\rangle$ and dropping the unimportant normalization factor, we get the state

$$|\psi_0\rangle\langle\psi_0| + O\left(2^n e^{-\beta\Delta} + \frac{2^n(\beta\|\hat{H}\|)^K}{K!}\right) \quad (29)$$

for the first register. In the equation above, the first term represents our targeted ground state $|\psi_0\rangle$, and there are two error terms: the first term comes from contribution of all the other eigenstates, shrunk by the imaginary time evolution factor $e^{-\beta\Delta}$ with Δ denoting the energy gap; and the second term comes from the truncation error in Taylor series expansion. Suppose we require the total representation error is bounded by a small constant ϵ , then we need

$$O(2^n e^{-\beta\Delta}) \leq \frac{\epsilon}{2}, \quad (30)$$

$$O\left(\frac{2^n(\beta\|\hat{H}\|)^K}{K!}\right) \leq \frac{\epsilon}{2}. \quad (31)$$

With an optimal choice of the parameter $\beta = O((n + \log(1/\epsilon))/\Delta)$, we need $K = O(\beta\|\hat{H}\|)$ to satisfy these inequalities. As $\|\hat{H}\| = O(m)$, we have $K = O((n + \log(1/\epsilon))m/\Delta)$. So the total number of elementary tensors we need to represent the ground state $|\psi_0\rangle$ of the Hamiltonian \hat{H} is given by $O(Km)$, which is

$$O\left(\frac{1}{\Delta} \left(n + \log \frac{1}{\epsilon}\right) m^2\right). \quad (32)$$

Each elementary tensor has a constant bond dimension D and a typically small coordination number d . Combining with theorem 3 in the main text, we find the total number of neurons in the DBM to represent the ground state of the Hamiltonian \hat{H} is also given by the above equation, which is the statement of theorem 4.